

Josai Mathematical Monographs  
vol. 9 (2016), pp. 31-42

# Numerical simulation of the behavior of three rising bubbles by an energy-stable finite element scheme

Masahisa TABATA

**Abstract.** We simulate numerically the behavior of three rising bubbles in a container. Each fluid is governed by the Navier-Stokes equations and the surface tension is considered on the interfaces. The simulation is carried out by an energy-stable finite element scheme developed by ourself. Merging of bubbles is also treated.

## 1. Introduction

Our purpose is to simulate numerically the behavior of three rising bubbles in a container. The mathematical formulation of this problem is as follows. We consider multi-fluid flow problems, where each fluid is governed by the Navier-Stokes equations and the surface tension proportional to the curvature acts on the interface. The domain which each fluid occupies is unknown, and the interface moves with the same velocity as the particle on it. While numerical solution of one-fluid flow problems governed by the Navier-Stokes equations has been successfully established from the point of stability and convergence, it is still not an easy task to devise numerical schemes solving the multi-fluid flow problems. To the best of our knowledge there are no numerical schemes whose solutions are proved to converge to the exact one and there is very little discussion even on the stability of schemes [1]. As for the study from the engineering point of view we refer to [3, 7] and the bibliography therein. For the multi-fluid flow problems we have developed a class of energy-stable finite element schemes in [4, 5], where they are proved to be stable in the sense of energy if a quantity corresponding to  $L^2$ -norm of the curvature remains bounded in the computation. Here we perform numerical simulation of the behavior of three rising bubbles by an energy-stable finite element scheme.

The contents of this paper are as follows. In Section 2 we present an energy-stable finite element scheme. In Section 3, after three-rising-bubble problem is stated, numerical simulation is performed. In Section 4 concluding remarks are given.

## 2. An energy-stable finite element scheme

Let  $\Omega$  be a bounded domain in  $\mathbf{R}^2$  with piecewise smooth boundary  $\Gamma$ , and  $(0, T)$  a time interval. The domain  $\Omega$  is occupied by  $m+1$  immiscible incompressible

viscous fluids. Each fluid  $k$ , whose density and viscosity are  $\rho_k$  and  $\mu_k$ , occupies an unknown domain  $\Omega_k(t)$  at time  $t$ . Fluid  $k(= 1, \dots, m)$  is surrounded by fluid 0, and the surface tension acts on the interface  $\Gamma_k(t)$ . Let the coefficient of the surface tension be  $\sigma_k$ .  $\Gamma_k(t)$  is expressed as a closed curve,

$$\Gamma_k(t) = \{\chi_k(s, t); s \in [0, 1]\},$$

where

$$\chi_k : [0, 1] \times (0, T) \rightarrow \mathbb{R}^2, \quad \chi(1, t) = \chi(0, t) \quad (t \in (0, T))$$

is a function to be determined.  $\Omega_k(t)$ ,  $k = 1, \dots, m$ , is the interior of  $\Gamma_k(t)$ , and fluid 0 occupies

$$\Omega_0(t) = \Omega \setminus \bigcup \{\bar{\Omega}_k(t); k = 1, \dots, m\}.$$

Unknown functions  $(u, p)$ , velocity and pressure,

$$u : \Omega \times (0, T) \rightarrow \mathbb{R}^2, \quad p : \Omega \times (0, T) \rightarrow \mathbb{R}$$

and  $\chi_k$  satisfy the system of equations,

$$\rho_k \left\{ \frac{\partial u}{\partial t} + (u \cdot \nabla)u \right\} - \nabla [2\mu_k D(u)] + \nabla p = \rho_k f, \quad x \in \Omega_k(t), \quad t \in (0, T) \quad (1a)$$

$$\nabla \cdot u = 0, \quad x \in \Omega_k(t), \quad t \in (0, T) \quad (1b)$$

$$[u] = 0, \quad [-pn + 2\mu D(u)n] = \sigma_k \kappa n, \quad x \in \Gamma_k(t), \quad t \in (0, T) \quad (1c)$$

$$\frac{\partial \chi_k}{\partial t} = u(\chi_k, t), \quad s \in [0, 1], \quad t \in (0, T) \quad (1d)$$

$$u \cdot n = 0, \quad D(u)n \parallel n, \quad x \in \Gamma, \quad t \in (0, T) \quad (1e)$$

$$u = u^0, \quad x \in \Omega, \quad t = 0 \quad (1f)$$

$$\chi_k = \chi_k^0, \quad s \in [0, 1], \quad t = 0, \quad (1g)$$

where  $k = 0, \dots, m$  in (1a) and (1b),  $k = 1, \dots, m$  in (1c), (1d) and (1g), and

$$f : \Omega \times (0, T) \rightarrow \mathbb{R}^2, \quad u^0 : \Omega \rightarrow \mathbb{R}^2, \quad \chi_k^0 : [0, 1] \rightarrow \mathbb{R}^2$$

are given functions;  $f$  is an acceleration,  $u^0$  is an initial velocity,  $\chi_k^0$  is a function expressing the initial interface position.  $[\cdot]$  means the difference of the values approached from both sides to the interface,  $\kappa$  is the curvature of the interface, and  $n$  is the unit normal. On the boundary of  $\Omega$  the slip boundary condition (1e) is imposed.

Let  $X$ ,  $V$ ,  $Q$  and  $\Phi$  be function spaces defined by

$$\begin{aligned} X &= \left\{ \chi \in (H^1(0,1)^2)^m; \chi(1) = \chi(0) \right\}, \quad \Phi = L^\infty(\Omega), \\ V &= \left\{ v \in H^1(\Omega)^2; v \cdot n = 0 \text{ } (x \in \Gamma) \right\}, \quad Q = L^2_0(\Omega). \end{aligned}$$

Let  $X_h$ ,  $\Phi_h$ ,  $V_h$  and  $Q_h$  be finite-dimensional approximation spaces of  $X$ ,  $\Phi$ ,  $V$  and  $Q$ . Let  $\Delta t$  be a time increment and  $N_T = \lfloor T/\Delta t \rfloor$ . At  $t = n\Delta t$  we seek an approximate solution  $(\chi_h^n, \rho_h^n, \mu_h^n, u_h^n, p_h^n)$  in  $X_h \times \Phi_h \times \Phi_h \times V_h \times Q_h$ . More precisely, these approximate function spaces are constructed as follows. Dividing the domain  $\Omega$  into a union of triangles, we use  $P1$ ,  $P2$  and  $P1$  finite element spaces for  $\Phi_h$ ,  $V_h$  and  $Q_h$ , respectively. They are fixed for all time steps  $n$ . On the other hand,  $X_h$  is composed of functions obtained by the parameterization of polygons. We denote by  $\{s_i^{k,n} \in [0,1]; i = 0, \dots, N_x^{k,n}\}$  the set of parameter values such that  $s_0^{k,n} = 0$  and  $s_{N_x^{k,n}}^{k,n} = 1$  and that  $\{\chi_{hk}^n(s_i^{k,n}); i = 0, \dots, N_x^{k,n} - 1\}$  is the set of vertices of the  $k$ -th polygon for  $k = 1, \dots, m$ . The number  $N_x^{k,n}$  may change depending on  $k$  and  $n$ . We denote  $\{N_x^{k,n}\}_{k=1}^m$  by  $N_x^n$ . Our scheme is to find

$$\{(\chi_h^n, \rho_h^n, \mu_h^n, u_h^n, p_h^n) \in X_h \times \Phi_h \times \Phi_h \times V_h \times Q_h; n = 1, \dots, N_T\}$$

satisfying

$$\begin{aligned} \frac{\tilde{\chi}_{hk}^n - \chi_{hk}^{n-1}}{\Delta t} &= \\ \begin{cases} u_h^{n-1}(\chi_{hk}^{n-1}), & \forall s_i^{k,n-1}, n = 1 \\ \frac{3}{2}u_h^{n-1}(\chi_{hk}^{n-1}) - \frac{1}{2}u_h^{n-2}(\chi_{hk}^{n-1} - \Delta t u_h^{n-1}(\chi_{hk}^{n-1})), & \forall s_i^{k,n-1}, n \geq 2, \end{cases} \end{aligned} \quad (2a)$$

$$\chi_h^n = \mathcal{X}_h(\tilde{\chi}_h^n), \quad \rho_h^n = \mathcal{R}_h(\chi_h^n), \quad \mu_h^n = \mathcal{M}_h(\chi_h^n), \quad (2b)$$

$$\begin{aligned} & \left( \rho_h^{n-1} \bar{D}_{\Delta t} u_h^n + \frac{1}{2} u_h^n \bar{D}_{\Delta t} \rho_h^n, v_h \right) + a_1(\rho_h^n, u_h^{n-1}, u_h^n, v_h) + a_0(\mu_h^n, u_h^n, v_h) \\ & + b(v_h, p_h^n) + \Delta t \, d_h(u_h^n, v_h; \mathcal{C}_h^n) = (\rho_h^n \Pi_h f^n, v_h) - d_h(\chi_h^n, v_h; \mathcal{C}_h^n), \\ & \qquad \qquad \qquad \forall v_h \in V_h, \end{aligned} \quad (2c)$$

$$b(u_h^n, q_h) = 0, \quad \forall q_h \in Q_h \quad (2d)$$

subject to the initial conditions

$$\chi_h^0 = \Pi_h \chi^0, \quad \rho_h^0 = \mathcal{R}_h(\chi_h^0), \quad \mu_h^0 = \mathcal{M}_h(\chi_h^0), \quad u_h^0 = \Pi_h u^0, \quad (3)$$

where  $\Pi_h$  is the Lagrange interpolation operator to the corresponding finite-dimensional space. Equations (2a)-(2d) are composed of the four stages.

Stage 1. Let  $(\chi_h^{n-1}, u_h^{n-1}, u_h^{n-2}) \in X_h(N_x^{n-1}) \times V_h \times V_h$  be given for  $n \geq 2$ . When  $n = 1$ ,  $(\chi_h^0, u_h^0) \in X_h(N_x^0) \times V_h$  is given by (3). By (2a) we get a temporary

function  $\tilde{\chi}_h^n$ ,

$$\begin{aligned} (\chi_h^{n-1}, u_h^{n-1}, u_h^{n-2}) &\rightarrow \tilde{\chi}_h^n \in X_h(N_x^{n-1}), \quad n \geq 2 \\ (\chi_h^0, u_h^0) &\rightarrow \tilde{\chi}_h^1 \in X_h(N_x^0), \quad n = 1. \end{aligned}$$

(2a) is the Adams-Bashforth approximation of (1d) for  $n \geq 2$ , and the forward Euler approximation for  $n = 1$ .

Stage 2. By (2b) we fix a function  $\chi_h^n$ ,

$$\tilde{\chi}_h^n \rightarrow \chi_h^n \in X_h(N_x^n).$$

Here we modify  $\tilde{\chi}_{hk}^n$  to have a quasi-uniform distribution of vertices of the polygon  $\tilde{\mathcal{C}}_{hk}^n$  associated with  $\tilde{\chi}_{hk}^n$  and to keep the area of the surrounded domain to be equal to the initial area. Those all procedures are denoted by  $\mathcal{X}_h(\tilde{\chi}_h^n)$  in (2b).

Stage 3. By (2b) we obtain

$$\chi_h^n \rightarrow \rho_h^n \in \Phi_h$$

as follows. Once  $\chi_h^n$  is known, we can define  $\Omega_{hk}^n$  for all  $k$ . If the node  $P_i$  belongs to  $\Omega_{hk}^n$ , we set

$$\rho_h^n(P_i) = \rho_k.$$

This procedure is denoted by  $\mathcal{R}_h(\chi_h^n)$ . Similarly,  $\mathcal{M}_h(\chi_h^n)$  is defined.

Stage 4. By solving a system of linear equations, (2c) and (2d), we get  $u_h^n$  and  $p_h^n$ ,

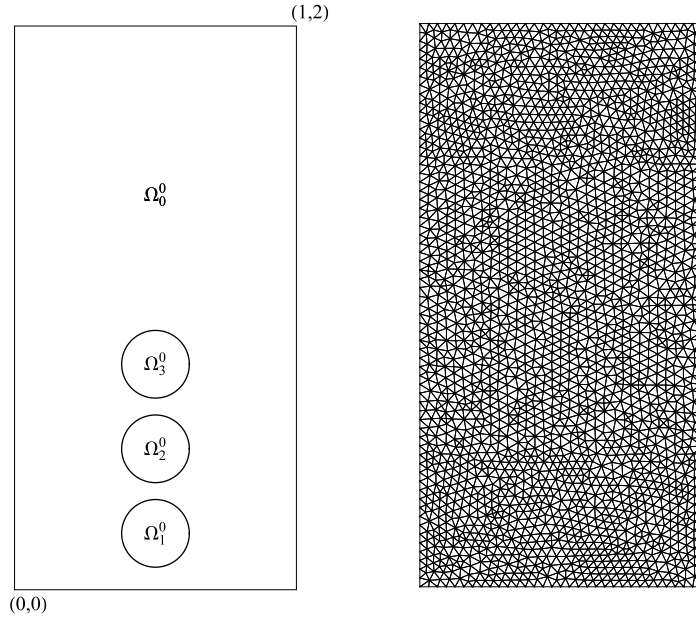
$$(\chi_h^n, \rho_h^n, \rho_h^{n-1}, \mu_h^n, u_h^{n-1}) \rightarrow (u_h^n, p_h^n) \in V_h \times Q_h.$$

In (2c) the symbol  $(\cdot, \cdot)$  shows the inner product in  $L^2(\Omega)^2$  and  $\bar{D}_{\Delta t}$  is the backward difference with respect to  $\Delta t$ . The linear forms  $a_1$ ,  $a_0$ ,  $b$ , and  $d_h$  are defined by

$$\begin{aligned} a_1(\rho, w, u, v) &= \int_{\Omega} \frac{1}{2} \rho \left\{ [(w \cdot \nabla)u] \cdot v - [(w \cdot \nabla)v] \cdot u \right\} dx, \\ a_0(\mu, u, v) &= \int_{\Omega} 2\mu D(u) : D(v) \, dx, \quad b(v, q) = - \int_{\Omega} (\nabla \cdot v) q \, dx, \\ d_h(u, v; \mathcal{C}_h) &= \sum_{k=1}^m \sigma_k \sum_{i=1}^{N_x^k} \bar{D}_{\Delta s} u_i \cdot \bar{D}_{\Delta s} v_i \frac{(s_i^k - s_{i-1}^k)^2}{|\chi_{hk}(s_i^k) - \chi_{hk}(s_{i-1}^k)|}, \end{aligned} \tag{4}$$

where  $\mathcal{C}_h$  is the set of  $k$  polygons associated with  $\chi_h$ ,  $\bar{D}_{\Delta s}$  is the backward difference with respect to the parameter  $s$ . For more details of this scheme refer to [5], where the following advantages are also shown.

- It is stable in the sense of energy if a summation of the square of approximate

Figure 1. Domain  $\Omega$  and mesh  $\mathcal{T}_h$ .

curvature of the interface remains bounded.

- Since we use the interface-tracking method, we can distribute much more nodes on the interface than the level-set method.
- When it is applied to incompressible viscous one-fluid flow problems, the stability and convergence is assured.
- Since the main computation part is similar to that of the Stokes problem, the computation cost is small.

We apply this scheme to our problem.

### 3. Numerical simulation of three-rising-bubble problem

#### 3.1. Statement of the problem

Let  $m = 3$  and we consider the domain  $\Omega$  and three bubbles shown in Fig. 1 (left), where

$$\begin{aligned}\Omega &= (0, 1) \times (0, 2), \\ \Omega_1^0 &= \{(x_1, x_2); (x_1 - 0.5)^2 + (x_2 - 0.2)^2 < r^2\}, \quad r = 0.12, \\ \Omega_2^0 &= \{(x_1, x_2); (x_1 - 0.5)^2 + (x_2 - 0.5)^2 < r^2\},\end{aligned}$$

$$\Omega_3^0 = \{(x_1, x_2); (x_1 - 0.5)^2 + (x_2 - 0.8)^2 < r^2\}.$$

We set

$$\rho_0 = 100, \mu_0 = 2.0, u^0 = (0, 0)^T, f = (0, -1)^T, T = 10.$$

As for the densities of the bubbles we consider two cases:

$$(\rho_1, \rho_2, \rho_3) = (0.1, 10.0, 19.9), \quad (5a)$$

$$(\rho_1, \rho_2, \rho_3) = (19.9, 10.0, 0.1), \quad (5b)$$

and the other constants are

$$\mu_i = 1.0, \sigma_i = 1.0, \quad (i = 1, 2, 3).$$

In (5a) the densities of the lower bubbles are smaller, and in (5b) they are larger. When the interface curves of two bubbles intersect, two bubbles merge to become a big bubble with the average density. Then,  $m$  decreases by 1.

Fig. 1(right) shows the mesh  $\mathcal{T}_h$  used in the computation. The total number  $N_e$  of elements, the representative element size  $h$  are

$$N_e = 4,564, \quad h = 1/32.$$

The time increment  $\Delta t$  and the total time step  $N_T$  are

$$\Delta t = 1/32 \quad N_T = 320.$$

### 3.2. The case (5a)

Fig. 2 shows the time history of interfaces and streamlines from  $t = 0$  until 8.75. Three bubbles, which are put at the equi-distance at  $t = 0$ , begin to rise up and streamlines appear. Since the densities have the relation  $\rho_1 < \rho_2 < \rho_3$ , the lower bubbles rise up faster than the upper bubbles. Fig. 3 shows the detail time history of interfaces and streamlines from  $t = 4.0625$  until 6.5625. At first, bubbles 2 and 3 merge, and afterwards bubble 1 merges into a big bubble. Due to the surface tension the shape of the interface becomes round. Finally, the bubble stops at the ceiling and the streamlines disappear, that is, the stationary state arrives.

### 3.3. The case (5b)

Fig. 4 shows the time history of interfaces and streamlines from  $t = 0$  until 8.75. Three bubbles, which are put at the equi-distance at  $t = 0$ , begin to rise up. Since the densities have the relation  $\rho_3 < \rho_2 < \rho_1$ , the upper bubbles rise up faster than the lower bubbles. The distances of each two bubbles increase for a while. Finally, however, three bubbles merge into a big bubble since there is the ceiling. Fig. 5 shows the detail time history of interfaces and streamlines from  $t = 4.6875$

until 7.1875. At first, bubbles 2 and 3 merge in to a bubble, whose shape becomes smooth gradually in the effect of the surface tension. At  $t = 8.75$  bubble 1 does not yet merge into a big bubble, but later it merges.

#### 4. Concluding remarks

We have performed numerical simulation of the behavior of three rising bubbles in two cases (5a) and (5b). Merging of bubbles is carried out simply when two interface curves intersect each other. The system of linear equations in  $(u_h^n, p_h^n)$  to be solved in scheme (2) is asymmetric. This system can become symmetric if the Lagrange-Galerkin approximation [2, 6] is applied.

**Acknowledgments.** The author was supported by JSPS (Japan Society for the Promotion of Science) under Grants-in-Aid for Scientific Research (C), No. 25400212 and (S), No. 24224004 and under the Japanese-German Graduate Externship (Mathematical Fluid Dynamics) and by Waseda University under Project research, Spectral analysis and its application to the stability theory of the Navier-Stokes equations of Research Institute for Science and Engineering.

#### References

- [1] Bänsch, C: Finite element discretization of the Navier-Stokes equations with a free capillary surface. *Numer. Math.* **88**, 203–235, (2001).
- [2] Notsu, H and Tabata, M: Error estimates of a stabilized Lagrange-Galerkin scheme for the Navier-Stokes equations, *ESAIM: Mathematical Modelling and Numerical Analysis*, DOI: <http://dx.doi.org/10.1051/m2an/2015047>.
- [3] Prosperetti, A. and Tryggvason, G.: *Computational Methods for Multiphase Flow*. Cambridge University Press, Cambridge (2009).
- [4] Tabata, M: Finite element schemes based on energy-stable approximation for two-fluid flow problems with surface tension. *Hokkaido Math. J.* **36**, 875–890 (2007).
- [5] Tabata, M.: Numerical simulation of fluid movement in an hourglass by an energy-stable finite element scheme. In Hafez, M. N., Oshima, K. and Kwak, D. (eds) *Computational Fluid Dynamics Review 2010*, pp. 29–50. World Scientific, Singapore (2010).
- [6] Tabata, M.: Numerical simulation of the behavior of a rising bubble by an energy-stable Lagrange-Galerkin scheme, to appear in the *Proceedings of AFSI 2004, Modeling and Simulation in Science, Engineering and Technology Book Series*, Springer.
- [7] Tezduyar, T. E., Behr, M. and Liou, J.: A new strategy for finite element computations involving boundaries and interfaces - the deforming-spatial-domain /space-time procedure: I. *Comput. Methods Appl. Mech. Engrg.* **94**, 339–351 (1992).

Masahisa Tabata

Department of Mathematics, Faculty of Science and Engineering, Waseda University  
3-4-1, Ohkubo, Shinjuku, Tokyo, 169-8555 Japan  
tabata@waseda.jp



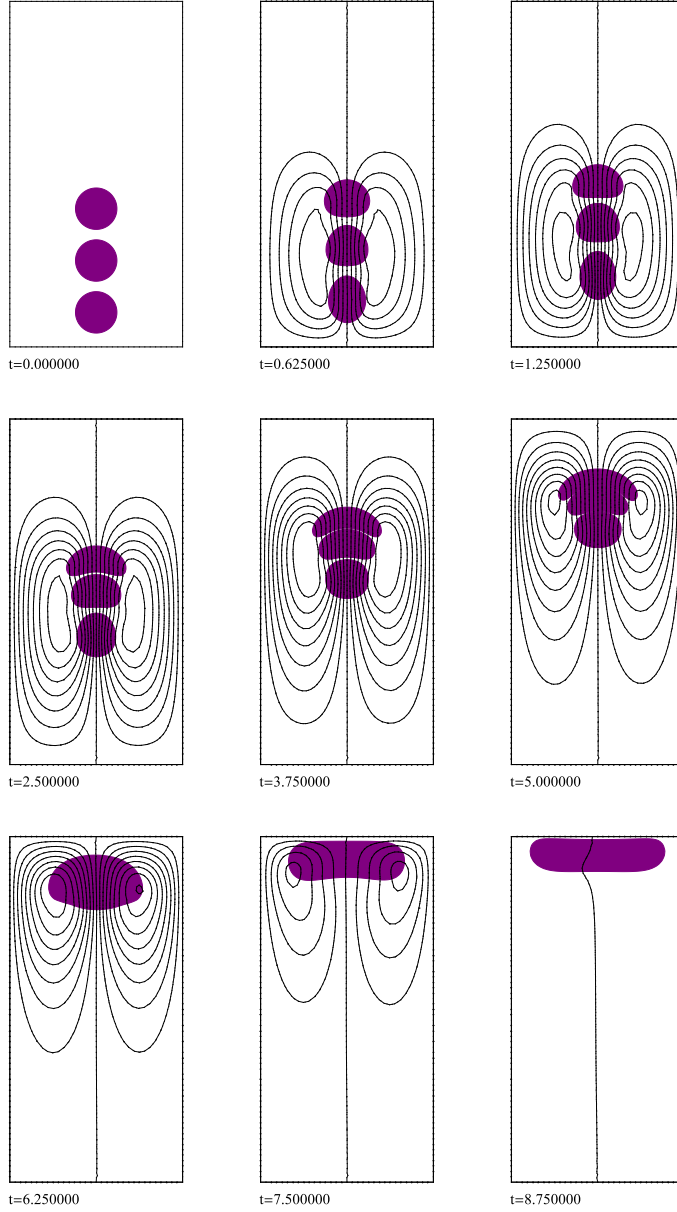


Figure 2. Interfaces and streamlines in the case (5a) from  $t = 0$  until 8.75.

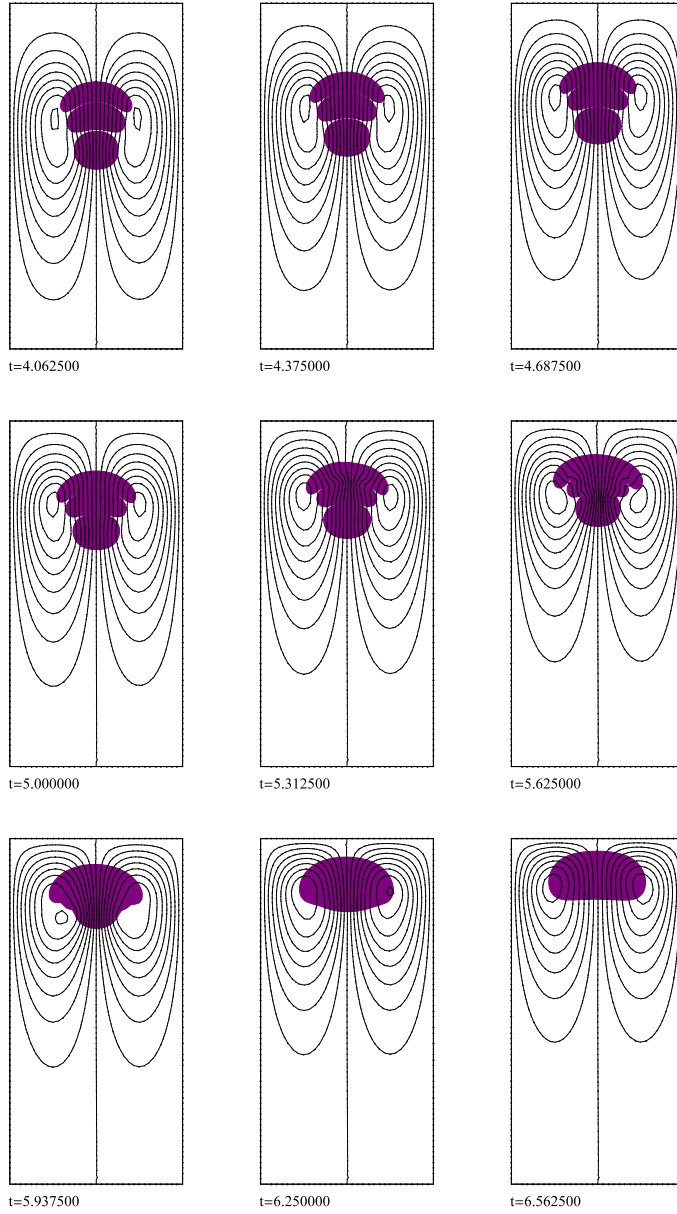


Figure 3. Interfaces and streamlines in the case (5a) from  $t=4.0625$  until  $6.5625$ .

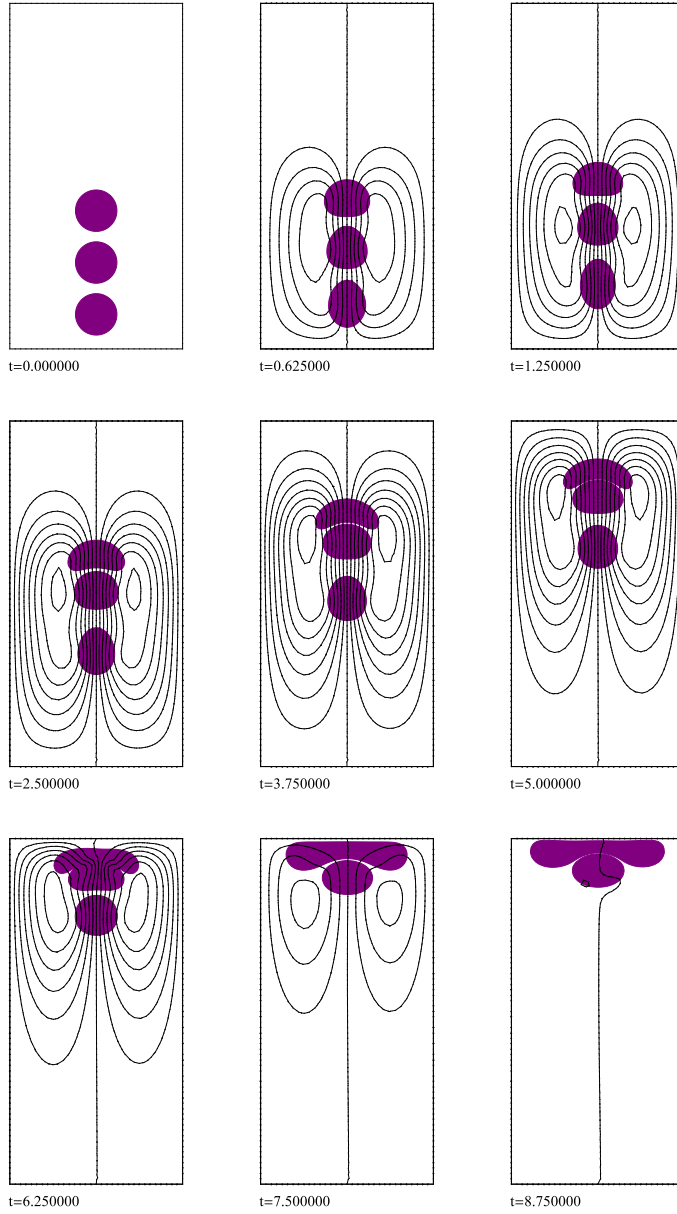


Figure 4. Interfaces and streamlines in the case (5b) from  $t = 0$  until 8.75.

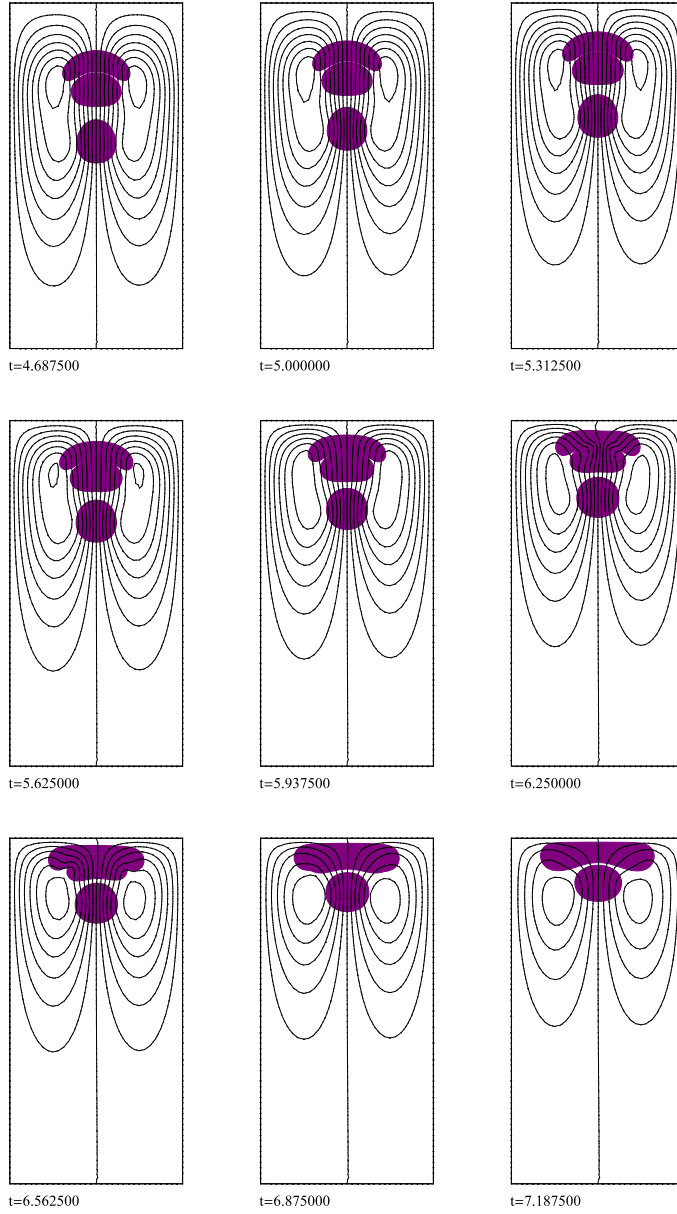


Figure 5. Interfaces and streamlines in (5b) from  $t=4.6875$  until  $7.1875$